NACA RM L52C18

NACA

RESEARCH MEMORANDUM

AN EXPERIMENTAL INVESTIGATION OF THE ZERO-LIFT PRESSURE DISTRIBUTION OVER A WEDGE AIRFOIL IN CLOSED, SLOTTED, AND OPEN-THROAT TUNNELS AT TRANSONIC MACH NUMBERS

By William J. Nelson and Frederick Bloetscher

Langley Aeronautical Laboratory
Langley Field, Va.

NATIONAL ADVISORY COMMITTEE
FOR AERONAUTICS

WASHINGTON
June 16, 1952

NATIONAL ADVISORY COMMITTEE FOR AERONAUTICS

RESEARCH MEMORANDUM

AN EXPERIMENTAL INVESTIGATION OF THE ZERO-LIFT PRESSURE DISTRIBUTION OVER A WEDGE AIRFOIL IN CLOSED, SLOTTED, AND OPEN-THROAT TUNNELS AT TRANSONIC MACH NUMBERS

By William J. Nelson and Frederick Bloetscher

SUMMARY

Pressure distributions and schlieren photographs of the flow about a 10-percent-thick diamond airfoil at zero lift in two-dimensional closed, slotted, and open-throat tunnels are presented and discussed. Uncorrected airfoil pressures obtained in $\frac{1}{5}$- and $\frac{1}{8}$-open slotted throat tunnels are compared at subsonic Mach numbers with corrected results from open and closed test sections of the same dimensions. The effect of varying the slot width has been investigated at Mach numbers up to 0.92. At Mach numbers up to 1.18, data obtained in test sections whose upper and lower boundaries were slotted to provide openings the combined width of which was equal to one-eighth of the tunnel width, are shown to be consistent with theory and available experiments.

INTRODUCTION

The removal of the choking limitation of conventional closed throat tunnels by the introduction of longitudinal slots in the tunnel boundaries makes possible the testing of relatively large models throughout the transonic range. Previous investigations have shown that slotting of the test section walls also effects substantial reductions in the jet-boundary interference effects (references 1 to 3). The current investigation, conducted in the Langley Internal Aerodynamics Section, is part of the continuing research on the problems of boundary interference in transonic tunnels. In conducting this research an airfoil whose chord was eight-ninths of the tunnel height has been used to amplify the boundary interference effects although the airfoil is much larger than would normally be considered appropriate for wind-tunnel testing.

Reported herein are the results of two-dimensional tests of a nonlifting symmetrical wedge airfoil in a tunnel whose upper and lower boundaries were closed, open, or slotted. In the slotted configuration, three different slot arrangements were used. Chordwise pressure distributions obtained from tests in each of the slotted wall configurations are presented without correction and compared with both uncorrected and corrected subsonic results of tests in open and closed jets of the same size. Comparisons of the pressure-drag curves from each facility and of schlieren photographs of the flow in the vicinity of the airfoil are also presented. Tests at supersonic Mach numbers, M = 1.02 to 1.18, were made in only one of the slotted configurations; surface pressure distributions obtained in these tests are compared with the calculated results of references 4 and 5 and with available experiment.

SYMBOLS

c	model chord
D	pressure drag per unit surface area
h	tunnel height, distance between upper and lower walls of jet
M	Mach number in model plane based on tunnel calibration
P	static pressure
t	airfoil maximum thickness
w	tunnel width
x	distance along chord from leading edge
y	distance from tunnel center line, measured along the airfoil span
C_D	drag coefficient of one-half of front wedge
$\tilde{C}_D$	generalized drag coefficient, $\tilde{C}_D \approx \frac{(\gamma + 1)^{1/3}}{(t/c)^{5/3}} C_D$

ξ_o speed function, $\xi_o \approx \frac{M^2 - 1}{\left[(\gamma + 1)t/c\right]^{2/3}}$

γ ratio of specific heats for air

Subscripts:

f front wedge

o stagnation conditions

APPARATUS AND TESTS

The general arrangement of the tunnel test section used in this investigation is shown in the photograph of figure 1 with the diamond airfoil extended through the glass side walls. The $4\frac{1}{2}$- by $6\frac{1}{4}$-inch test section was enclosed within a 30-inch-diameter cylindrical chamber, the upper portion of which has been raised for the photograph. The contraction ratio in an entrance bell preceding the throat was 20:1. Details of the boundary configurations tested are presented in figure 2. The slot sizes and locations are presented in figure 2(a). Photographs of the tunnel with one side plate removed to show the model and several of the boundary configurations are presented in figures 2(b) to 2(e). The tunnel height was maintained constant from the inlet bell to the downstream diffuser in all configurations except the open jet; in this configuration the collector bell was 22 percent higher than the inlet section.

In all tests except those made in the $\frac{1}{8}$-open multiple-slotted throat, the air was supplied at room conditions with the downstream end of the chamber and test section open to the low-pressure source. In the tests using the $\frac{1}{8}$-open multiple-slotted throat, the stagnation temperature and pressure were raised to approximately 670° R and 1.25 atmosphere absolute, respectively, and a vacuum pump was attached to the surrounding chamber to provide the pressure difference required to generate supersonic Mach numbers as discussed in reference 6. The test-section Mach number was determined from tunnel-empty surveys of the airfoil position referenced in the closed tunnel to the wall static pressure at a point approximately 0.6 chord ahead of the model and in the slotted- and open-throat tests to the static pressure in the chamber.

The model used in this investigation was a 10-percent-thick diamond-shaped airfoil with a 4-inch chord and an 11-inch span. The model was

mounted on the tunnel center line and supported in close fitting cut-outs in the glass side walls of the throat. Pressure orifices 0.010 inch in diameter were located along the upper surface of the airfoil at x/c equal to 0.075, 0.15, 0.25, 0.30, 0.35, 0.40, 0.45, 0.488, 0.512, 0.55, 0.60, 0.65, 0.70, 0.75, 0.85, 0.925, and along the lower surface at x/c equal to 0.125, 0.25, 0.35, 0.45, 0.55, 0.65, 0.75, and 0.875. A single-pass schlieren optical system with a light exposure of approximately 5 microseconds was used to obtain photographs of the flow in the vicinity of the model.

The maximum Reynolds number of the tests, based on model chord, was on the order of 1.5×10^6; the maximum Mach number was 1.18. All tests were conducted with the model at an angle of attack of 0°.

RESULTS AND DISCUSSION

Effect of Slot Area Ratio

Schlieren photographs.- Schlieren photographs of the flow over the airfoil in the closed, multiple-slotted, and open test sections of equal size are presented for several subsonic free-stream Mach numbers in figures 3 to 6. In all of these photographs the direction of flow is from left to right; fuzziness along the surface of the airfoil results from spalling of the glass along the edge of the cut-out in which the model was supported. The direction of the light cut-off at the knife edge was such as to cause regions of compression to appear as areas of increased density in figures 3, 5, and 6; in figure 4 these regions appear as light areas.

In the closed throat tests (fig. 3), regions of increasing pressure are observed immediately after a region of rapid expansion at the mid-chord position at $M = 0.60$. With increasing stream Mach number lambda shocks develop in the region behind the 50-percent station on the wing and extend outward into the stream finally reaching the tunnel boundary at $M \cong 0.70$. (See fig. 3(d).) With the attainment of sonic velocity across the stream, as evidenced by the presence of shock waves spanning the jet, the choking Mach number of the tunnel was reached. (The choking Mach number based upon one-dimensional theory is 0.695. Excellent agreement of limiting Mach number, as determined by experiment and theory, appears to justify the selection of a station 0.6 chord ahead of the model as a reference for determining Mach number in this configuration.) Rearward movement of the normal shock at the limiting Mach number was effected by decreasing the tunnel back pressure. The thickness of the shock waves in these photographs is indicative of spanwise variations in velocity; these variations are probably confined to the ends of the

airfoil where the side-wall boundary layer effects a reduction in local Mach number. The regions of compression preceding the terminal shock waves are caused by the growth of the boundary layer over the surface of the airfoil and the reflection from the sonic line of the expansions originating just behind the midpoint of the airfoil. The disturbance which appears to originate on the upper surface of the airfoil at an x/c of approximately 0.8 is caused by imperfections of the spanwise joint in the airfoil. The wake of the airfoil is observed to increase in width and turbulence as the normal shock moves rearward until the shock moves off the trailing edge at which point the wake becomes relatively thin.

In the slotted and open-throat tunnels, the flow over the airfoil, as shown in the schlieren photographs of figures 4 to 6, undergoes a sequence of changes parallel to those observed in the closed throat tests (fig. 3). However, significant differences are observed in the indicated Mach number at which corresponding flow patterns were obtained in the various throat configurations. These differences in indicated Mach number increased with air speed. In each case the greatest indicated Mach number difference occurred between closed and open-throat tunnels.

Chordwise pressure distribution (subsonic).- Static pressures measured on the airfoil surface in the closed, slotted, and open-throat tunnel at $\frac{y}{w} = 0$ are presented in figures 7 to 10. These pressures, expressed in terms of upstream stagnation pressure, are plotted against chordwise distance from the leading edge of the airfoil. Pressures on the upper surface of the airfoil are designated by the plain symbols, those on the lower surface, by flagged symbols. In general, one curve is drawn through both sets of points; however, where the curves are widely separated, a dashed line is used to indicate the distribution along the lower surface.

Airfoil pressure distributions measured in the closed throat tests at Mach numbers from 0.50 to 0.70 are presented in figure 7. At Mach numbers below about 0.6 the flow over the entire airfoil was subsonic; in this range, the pressures over the upper and lower surface of the airfoil are in good agreement and the distribution nearly symmetrical about the midchord position. As the Mach number is increased beyond about 0.6, the flow expands rapidly through a Prandtl-Meyer turn at the midchord station establishing a region of supersonic flow which was terminated by compression shocks. The maximum local Mach number attained in the expansion increased from 1.0 at $M = 0.6$ to 1.4 at $M = 0.7$, the latter corresponds to a change in direction of flow of about 9° from the sonic velocity heading; the surface angle was 11.5°. The subsequent recompression occurs as a band of weak oblique shocks and a normal shock previously observed in the schlieren photographs. The

normal shock moves rearward with increasing Mach number and/or decreasing tunnel back pressure. Progressive rearward movement of the shock wave in the choked tunnel results in extension of the region of low pressures to the trailing edge of the airfoil; over the forward part of the airfoil, however, the pressure remained constant.

In the slotted- and open-throat-tunnel tests the pressures (figs. 8 to 10) measured over the airfoil surfaces at subcritical speeds behave in essentially the same manner as in the closed-throat tests. In these test sections, much higher Mach numbers were obtained than in the closed section and at these higher Mach numbers the pressure over the forward part of the airfoil decreased continuously with increasing Mach number as opposed to the attainment of a limiting value characteristic of choked, closed-throat tunnels. Thus slotting or opening the tunnel throat has changed the jet-boundary effects and eliminated the tunnel choking limitations; there remains, however, the problem of evaluating or cancelling the jet-boundary interference velocity.

The influence of the jet-boundary conditions on the pressures over the test airfoil are more clearly shown in figure 11 where the pressure-distribution curves for the various tunnels are superimposed at constant values of indicated Mach number; these curves were obtained by interpolation from figures 7 to 10. At Mach numbers of 0.5 and 0.6, pressures measured in the closed tunnel were appreciably lower than those obtained in the slotted and free-jet configurations, which among themselves showed only small differences. The differences between the closed-tunnel pressures and those measured in slotted and open tunnels increase with Mach number reaching a maximum at 0.7, the limiting speed of the closed tunnel. Over the front of the airfoil at Mach numbers above 0.7, pressures measured in the free-jet configuration were consistently lower than those measured in the slotted tunnels.

The preceding discussion of the jet-boundary influence has been qualitative and based entirely on uncorrected experimental data. In the absence of published pressure distributions from free-air tests of this profile, corrections have been applied to the closed- and open-jet results to obtain reference distributions at each of several Mach numbers. This correction was readily accomplished by proportioning the differences between open- and closed-tunnel experimental data at corresponding points, since the theoretical interference velocities in an open tunnel are numerically equal to one-half those for the corresponding closed tunnel and of opposite sign, a relationship which is independent of Mach number and body shape. A comparison of pressure distributions corrected by this method with uncorrected data from the $\frac{1}{8}$-open slotted-tunnel tests is presented in figure 12. The relative position of these curves suggests a difference in effective Mach number which at $M = 0.7$ is on the order of 3 percent.

Chordwise pressure distribution (sonic).- The chordwise pressure distribution at $M = 1.0$ for the 10-percent-thick symmetrical wedge profile has been calculated by Guderly and Yoshihara, reference 4. A comparison of experimental data from tests in the $\frac{1}{8}$-open slotted tunnel at $M \approx 1.0$ with these calculated results is presented in figure 13. The measured pressure gradients over the airfoil follow the calculated gradients closely. Small differences between measured and theoretical pressures over the front of the airfoil probably result from jet-boundary interference effects which are not completely eliminated by the slotted wall. Over the back of the airfoil the measured pressures are higher than those predicted by the theory. Part of this difference is attributed to the presence of the boundary layer which acts to reduce the change in direction of flow at the midpoint of the airfoil. Other experiments with this profile at Mach numbers close to unity have been conducted in the Langley annular transonic tunnel and in the Langley 4- by 19-inch tunnel. Data at $M = 1.0$ from these tests (reference 7 and unpublished, respectively) are also shown in figure 13. To avoid confusion of the experimental points from the different sources, these data are plotted on separate figures with the calculated distribution indicated on each plot to facilitate comparison. The consistency of the uncorrected data taken at $M = 1.0$ in a slotted test section whose height was only 11 percent greater than the wing chord with theory and with experimental data from experiments in test sections several times larger than the model is especially significant since it is at this point that subsonic theory predicts maximum boundary interference effects. Thus, by the use of a boundary with longitudinal slots whose combined area was one-eighth of the wall area, the jet-boundary effects on the nonlifting airfoil at subsonic speeds have been reduced to a point where in many applications they may be neglected.

Chordwise pressure distribution (supersonic).- As a transonic facility considerable interest is directed toward the slotted tunnel because in it a wide range of Mach numbers, supersonic as well as subsonic, may be realized without altering its geometry, whereas in closed- and open-jet tunnels, variable nozzle contour is required to change stream Mach number in the supersonic regime. Because the flow disturbance experienced at the model as a result of its proximity to the stream boundary was substantially smaller in the $\frac{1}{8}$-open slotted tunnel than in the other configurations tested, tests at supersonic Mach numbers were conducted in this configuration only.

Schlieren photographs of the flow over the airfoil at Mach numbers up to 1.18 are presented in figure 14; one picture at $M < 1.0$ is included for reference. At the supersonic Mach numbers the bow shock is detached and the flow approaching the airfoil is in all cases subsonic.

The position of the detached bow shock, visible in figures 14(e) and (f), is 0.1c to 0.2c further forward than would be expected from the calculations of Vincenti and Wagoner, reference 5; this difference is consistent with the fact that the calculations, based on a small perturbation theory and extrapolated to a 10-percent wedge by transonic similarity rules, indicate attachment of the bow shock at $M = 1.208$ whereas detached shocks are predicted by shock theory at all Mach numbers below 1.267. The shape of the detached wave over the middle third of the air stream is consistent with that of the calculated wave standing an equal distance ahead of the airfoil; however, the reverse curvature observed in the vicinity of the wall is caused by wall interference and has no counterpart in free air.

The transonic similarity laws have been applied to obtain from the generalized pressure distributions of reference 5, diagrams of P/P_o against x/c for Mach numbers of 1.05, 1.10, and 1.18. These are compared in figure 15 with the experimental data from $\frac{1}{8}$-open slotted-tunnel tests of the present investigation, figure 8. The general agreement of the calculated and experimental curves, although it does not constitute proof of the absence of jet-boundary interference effects in the $\frac{1}{8}$-open slotted tunnel in which these tests were made, is encouraging, especially in view of the extreme size of the model relative to the tunnel.

Pressure drag.- The airfoil drag, obtained by integration of the pressure diagrams presented previously are shown in figure 16 as a function of the indicated Mach number. A coefficient based on stagnation pressure rather than the dynamic pressure has been used to obtain a parameter which is independent of the boundary interference velocity. The spreading between these curves at low Mach numbers is attributed in a large measure to experimental inaccuracies and difficulties inherent in obtaining small differences between relatively large pressures over the front of the airfoil and those over the back. The rate of rise of the drag with Mach number is shown to be greatest in the closed tunnel as a result of choking at $M \approx 0.7$ decreasing progressively as amount of open boundary was increased.

Again in the absence of free-air data, reference curves have been obtained from interpolated closed- and open-tunnel data at subsonic Mach numbers ($M < 0.8$) and at sonic or supersonic Mach numbers from references 4 and 5. The lower drag obtained in the $\frac{1}{8}$-open slotted tunnel tests is a result of the higher pressures over the back of the airfoil. It is apparent from the pressure distributions of figure 13 that the drag obtained from experiments in the annular tunnel and the 4- by 19-inch tunnel will be similarly displaced from the theoretical value at $M = 1.0$. Tests on lifting wings in the $\frac{1}{8}$-open tunnel, reported in reference 3, were also in agreement with available experiments.

Tests of three simple wedges of semiapex angles $4\frac{1}{2}^{\circ}$, $7\frac{1}{2}^{\circ}$, and 10° at high subsonic and low supersonic Mach numbers have been reported by Liepmann and Bryson, reference 8. The semiapex angle of the front wedge used in the current investigation was 5.74°. The drag of one-half the front wedge as a function of Mach number is plotted in terms of transonic similarity parameters $\tilde{C}_{D_f}$ against ξ_o in figure 17, together with the results of reference 8 and the calculated curve from reference 5. The results from reference 8, plotted as an area rather than as individual points, may for all practical purposes be considered free from jet-boundary interference effects since the tunnel in which these tests were conducted was some 40 times the chord of the wedge. In the current slotted-tunnel tests, the jet height was 2.25 times the length of the front wedge. At $M = 1.0$ ($\xi_o = 0$), the results of the current investigation agree well with the calculations of reference 4; the slope of the curve, $d\tilde{C}_{D_f}/d\xi_o$, however, is somewhat lower than the calculated slope, reference 5. In those regions where these tests overlap those of reference 8, the same trends are observed although the values of $\tilde{C}_{D_f}$ from the current tests are higher than those of the reference. Part of this difference may be attributed to differences in afterbody configuration and differences in Reynolds number at which the data were taken as well as to boundary interference effects which are not completely eliminated by the slotted walls. Quantitative evaluation of the relative importance of these several sources of error is at present not feasible. It is apparent, however, that in the $\frac{1}{8}$-open slotted test section the jet-boundary interference velocities are small even though the model dimensions in relation to the tunnel size are far greater than would normally be considered practical.

Effect of Slot Spacing

Spanwise pressure distribution.- To investigate spanwise disturbances which might result from the nonhomogeneous nature of the slotted boundary, additional tests were conducted in a jet, the upper and lower walls of which contained single slots whose width was one-fifth that of the tunnel. At each of several chordwise stations data were taken in planes through the center of the slot and at the edge of the slot, over the closed part of the boundary near the side wall, and midway between the slot and side wall. Data taken on the upper surface of the airfoil, presented in figure 18, show the static-pressure variation with Mach number to be independent of spanwise location of the measuring station with the exception of points measured over the back of the airfoil in the vicinity of the side wall. These differences probably result from disturbances arising in the side-wall boundary layer rather than from any

effect of slot distribution. Thus it appears that the structural advantages of an installation with a small number of relatively large slots may be realized without incurring spanwise variations in boundary interference velocities. This conclusion, however, is based on subsonic tests ($M < 0.92$) and may not apply at higher speeds.

Chordwise pressure distribution.- The chordwise pressure distribution at the midspan station in the single-slotted tunnel, figure 19, followed the same general pattern with changing Mach number observed in all other configurations. In this test section, however, the direction of flow approaching the airfoil at Mach numbers of 0.8 or greater varied with Mach number causing substantial differences in pressure between corresponding points on the upper and lower surfaces. The magnitude and even the direction of these differences is observed to change with increasing Mach number. The experimental data obtained at $M = 0.60$, 0.80, and 0.92 are repeated in figure 20 where corresponding curves obtained from tests with the multiple-slotted boundaries are also presented. At $M = 0.60$, pressures in the single slotted jet are uniformly displaced below the curves from multiple-slotted configurations; thus it appears that the effective free area of the single slot is less than that of the many small slots. At higher Mach numbers, 0.80 and 0.92, the pressure over the forward part of the airfoil in the single-slotted configuration are consistent with curves from tests in multiple-slotted tunnels; at $\frac{x}{c} = 0.5 - 1.0$, however, the data lie on the closed tunnel side of the reference curves. Successful application of the larger slots, however, will require further refinement to obtain a more uniform stream.

Pressure drag.- The drag of the airfoil in the presence of single-slotted boundaries, obtained by integration of uncorrected pressure data, is shown in figure 21 as a function of stream Mach number together with similar curves from tests in multislot configurations. Again the effective slot area is observed to decrease as the slot size increases. From the relative position of these curves, the effective free-area ratio of the larger, single slot appears to be approximately one-half that of the uniformly distributed smaller slots. Without attempting an explanation of the differences in interference characteristics of single- and multiple-slotted boundaries of equal free area, it is pointed out that the increase in slot width was effected without an increase in depth; substantial differences in flow characteristics of the slots can therefore be expected, these will probably be accompanied by the development of much stronger vortices along the edge of the larger slots which are widely separated.

CONCLUSIONS

It is concluded from this experimental investigation of the zero-lift pressure distribution over a wedge airfoil in closed-, slotted-, and open-jet tunnels that:

1. In a $\frac{1}{8}$-open slotted tunnel the uncorrected pressures measured on a 10-percent-thick airfoil whose chord is eight-ninths of the tunnel height were in accord with available experiment and theory at Mach numbers up to 1.18.

2. Increasing the width of the individual slots while decreasing their number to maintain constant total slot area reduced the effective free area of the boundary.

3. When a single-slotted test section was used, the chordwise pressure distribution of the airfoil was found to be the same at all spanwise stations except those within 3/8 inch of the wall.

Langley Aeronautical Laboratory
National Advisory Committee for Aeronautics
Langley Field, Va.

REFERENCES

1. Wright, Ray H., and Ward, Vernon G.: NACA Transonic Wind-Tunnel Test Sections. NACA RM L8J06, 1948.

2. Ward, Vernon G., Whitcomb, Charles F., and Pearson, Merwin D.: An NACA Transonic Test Section with Tapered Slots Tested at Mach Numbers to 1.26. NACA RM L50B14, 1950.

3. Sleeman, William C., Jr., Klevatt, Paul L., and Linsley, Edward L.: Comparison of Transonic Characteristics of Lifting Wings from Experiments in a Small Slotted Tunnel and the Langley High-Speed 7- by 10-Foot Tunnel. NACA RM L51F14, 1951.

4. Guderley, Gottfried, and Yoshihara, Hideo: The Flow over a Wedge Profile at Mach Number One. Tech. Rep. No. 5783, ATI No. 57842, Air Materiel Command, U. S. Air Force, July 1949.

5. Vincenti, Walter G., and Wagoner, Cleo B.: Transonic Flow Past a Wedge Profile with Detached Bow Wave - General Analytical Method and Final Calculated Results. NACA TN 2339, 1951.

6. Nelson, William J., and Bloetscher, Frederick: Preliminary Investigation of a Variable Mach Number Two-Dimensional Supersonic Tunnel of Fixed Geometry. NACA RM L9D29a, 1949.

7. Habel, Louis W., and Henderson, James H.: Preliminary Investigation of Airfoil Characteristics in the Langley Annular Transonic Tunnel. NACA RM L50E18, 1950.

8. Liepmann, H. W., and Bryson, A. E., Jr.: Transonic Flow Past Wedge Sections. Jour. Aero. Sci., vol. 17, no. 12, Dec. 1950, pp. 745-755.

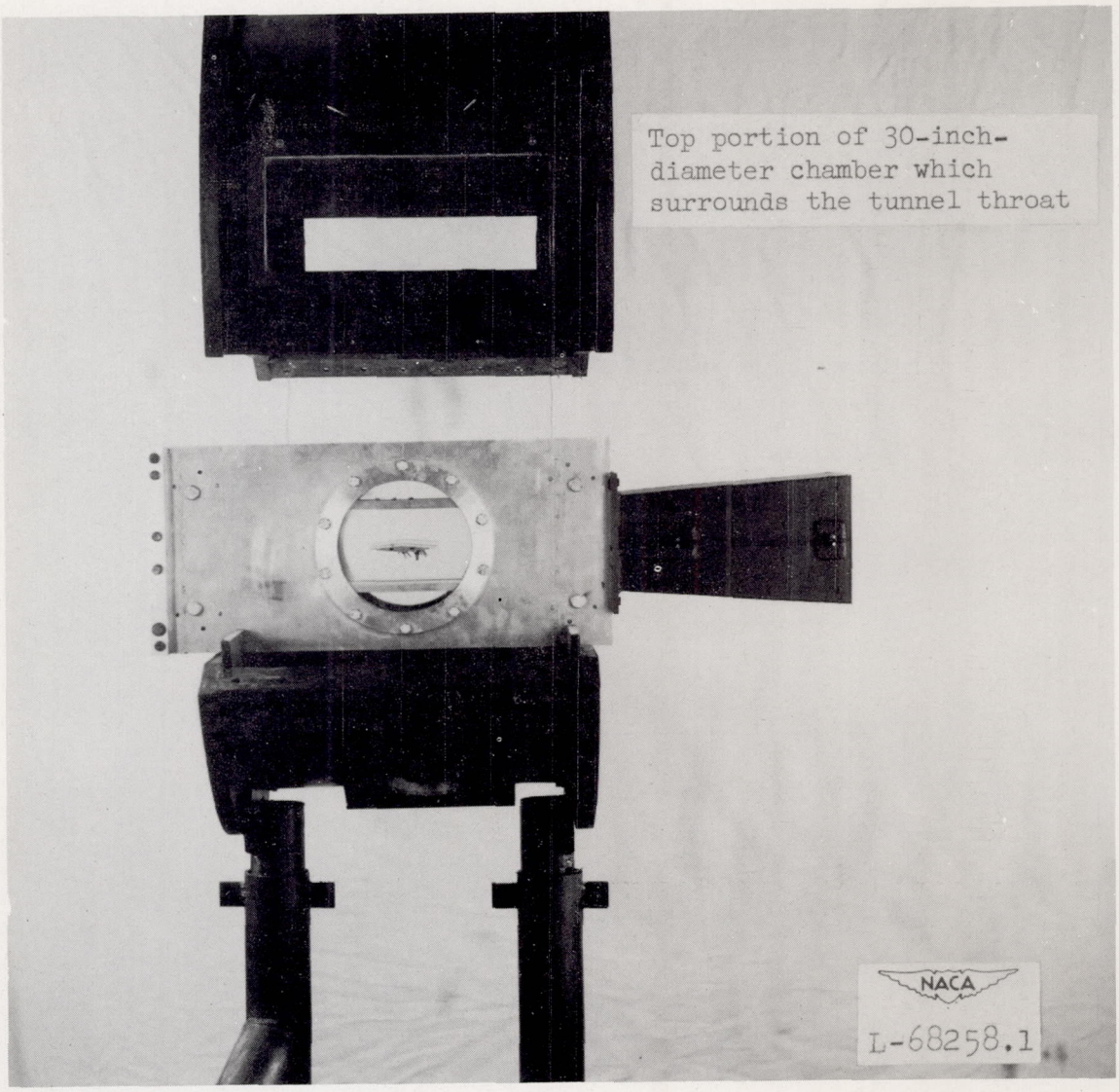

Figure 1.- General arrangement of tunnel test section and experimental model.

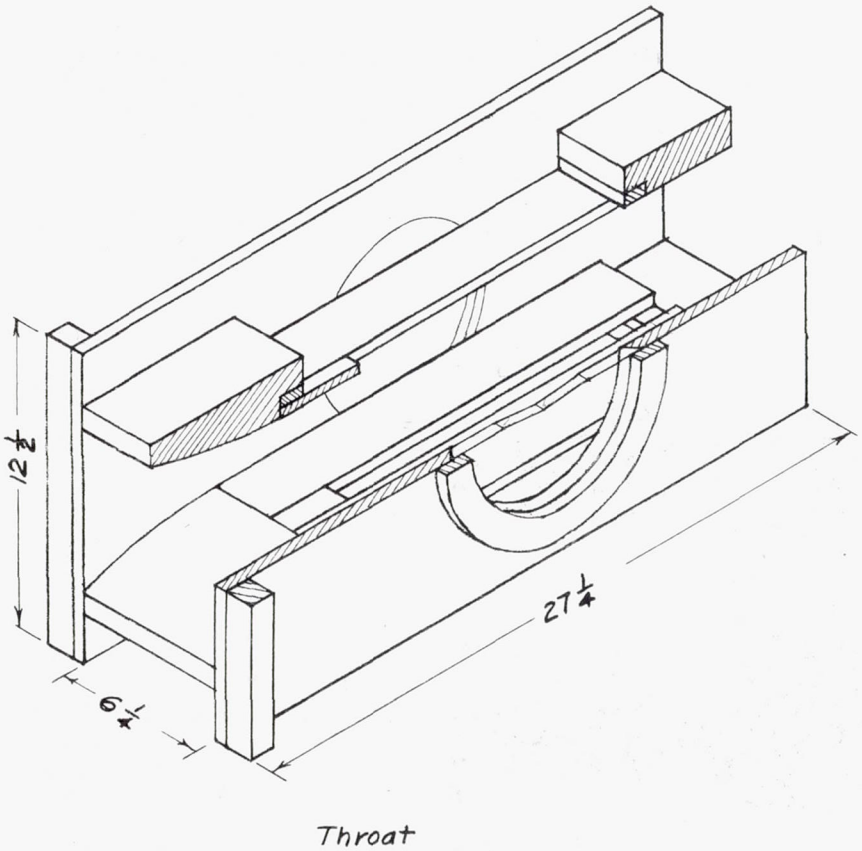

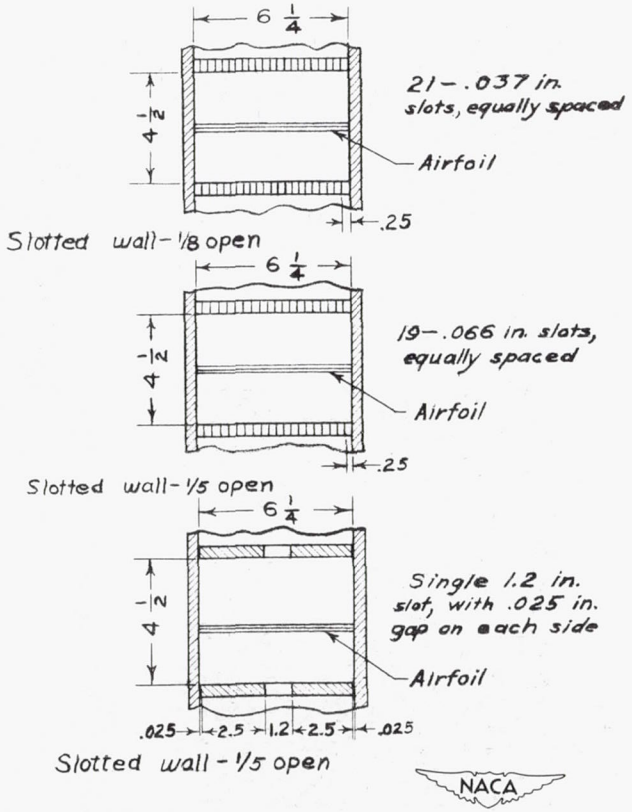

(a) Slotted-wall details.

Figure 2.- Test section and slotted walls. All dimensions are given in inches.

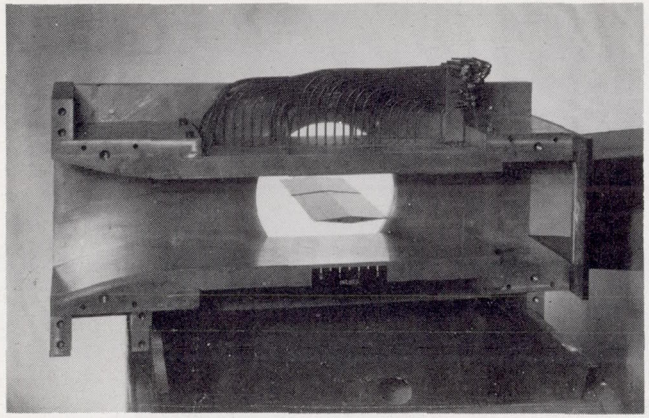

(b) Closed boundaries.

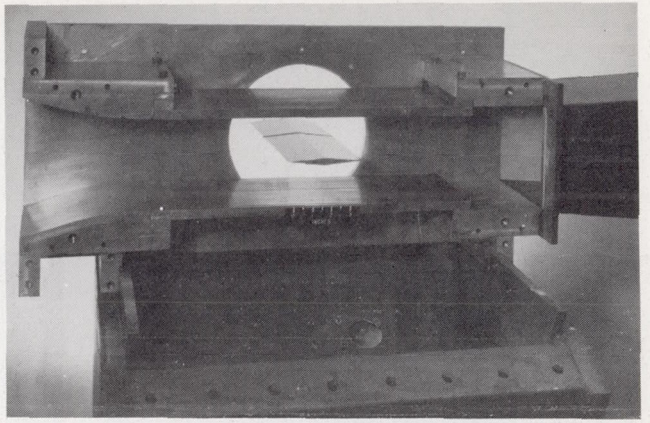

(c) Multiple slotted boundaries.

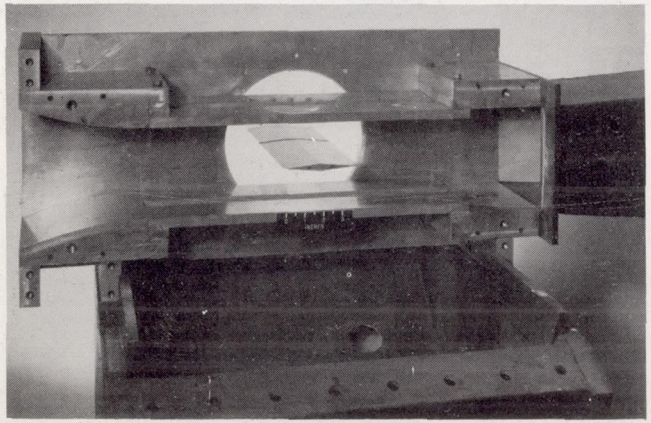

(d) Single-slotted boundaries.

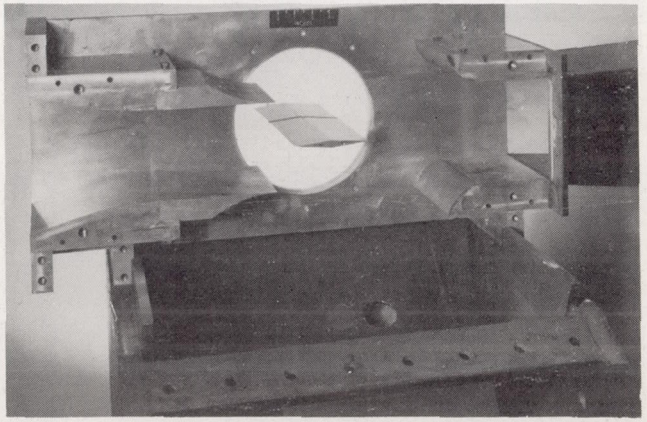

(e) Open jet boundaries.

Figure 2.- Concluded.

NACA

L-74350

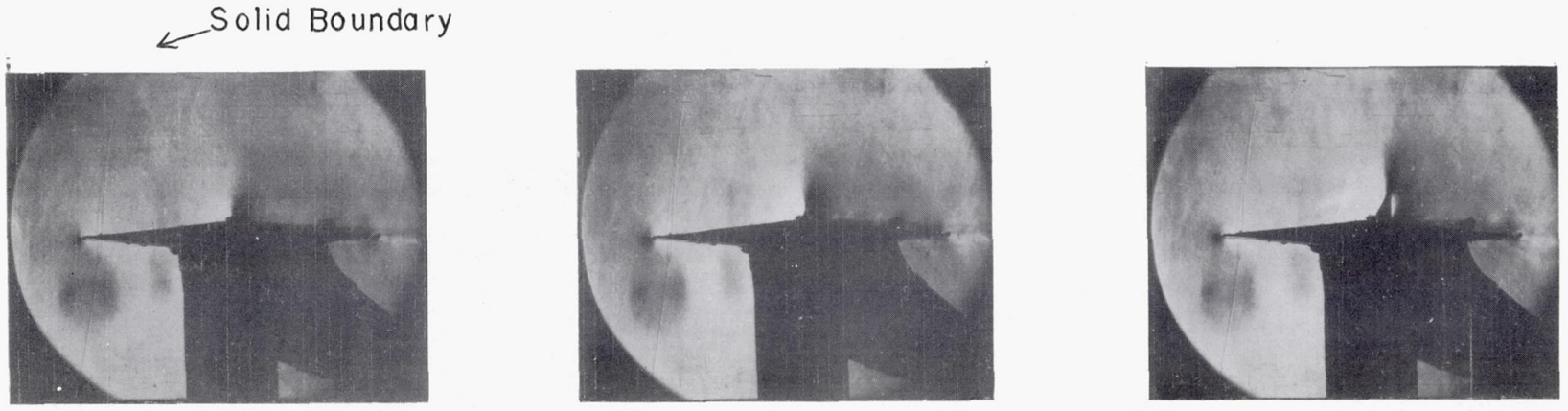

(a) M=0.60. (b) M=0.65. (c) M=0.68.

(d) M=0.70. (e) M=0.70. (f) M=0.70.

NACA

L-74351

Figure 3.- Schlieren photographs of flow over a 10-percent-thick diamond airfoil in the closed throat tunnel.

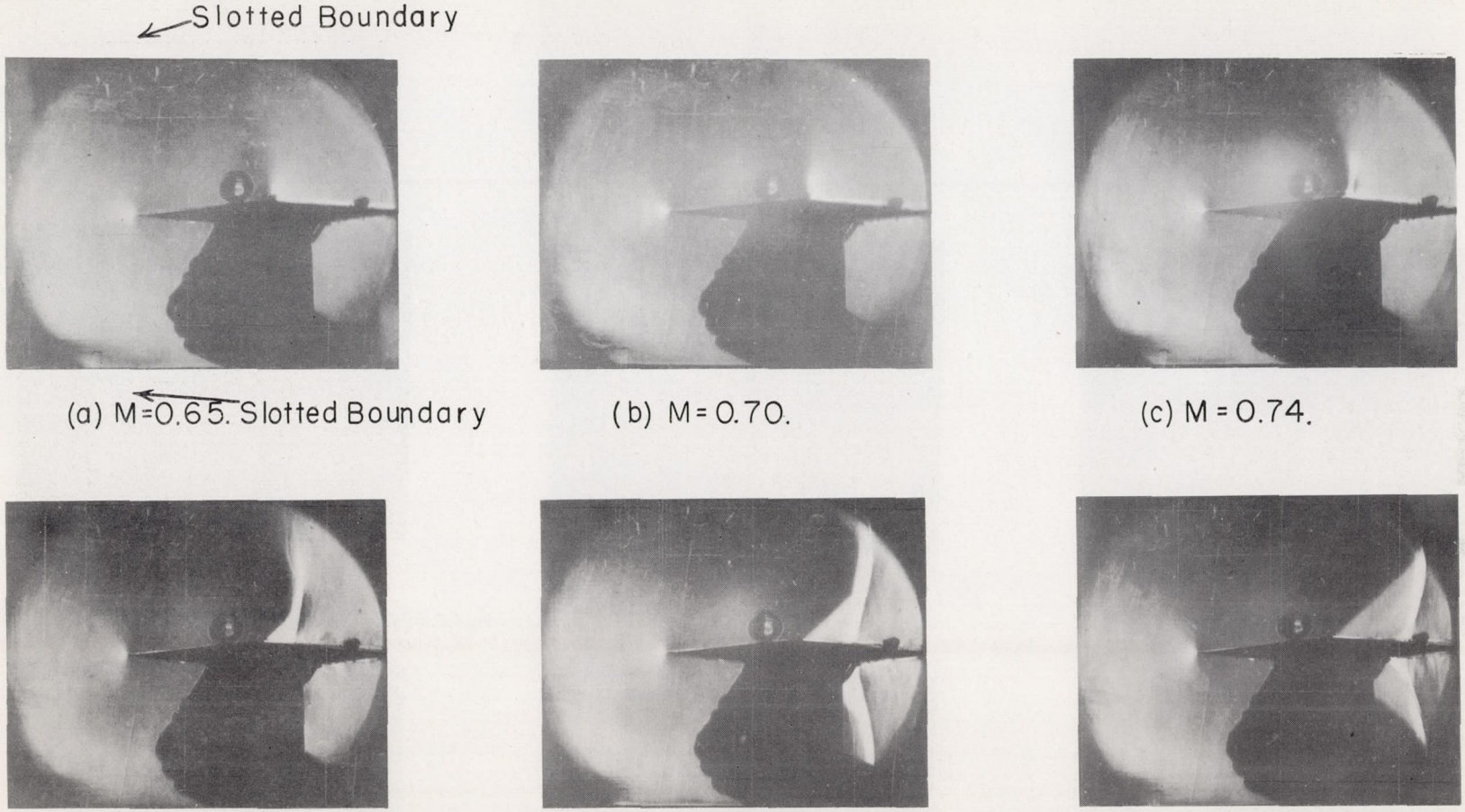

Figure 4.- Schlieren photographs of flow over a 10-percent-thick diamond airfoil in the $\frac{1}{8}$ - open multiple-slotted throat tunnel.

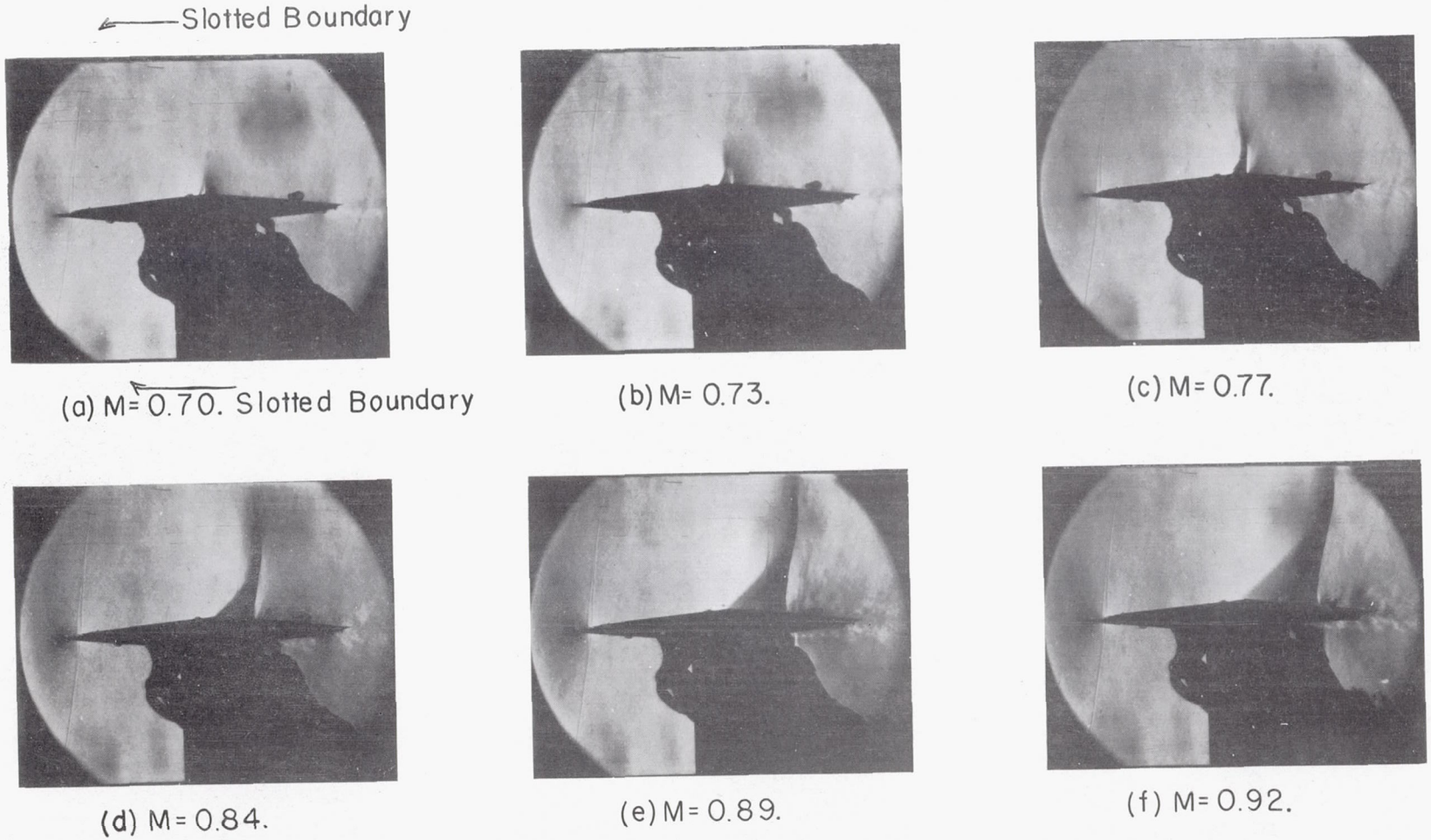

NACA

L-74353

Figure 5.- Schlieren photographs of flow over a 10-percent-thick diamond airfoil in the $\frac{1}{5}$-open multiple-slotted throat tunnel.

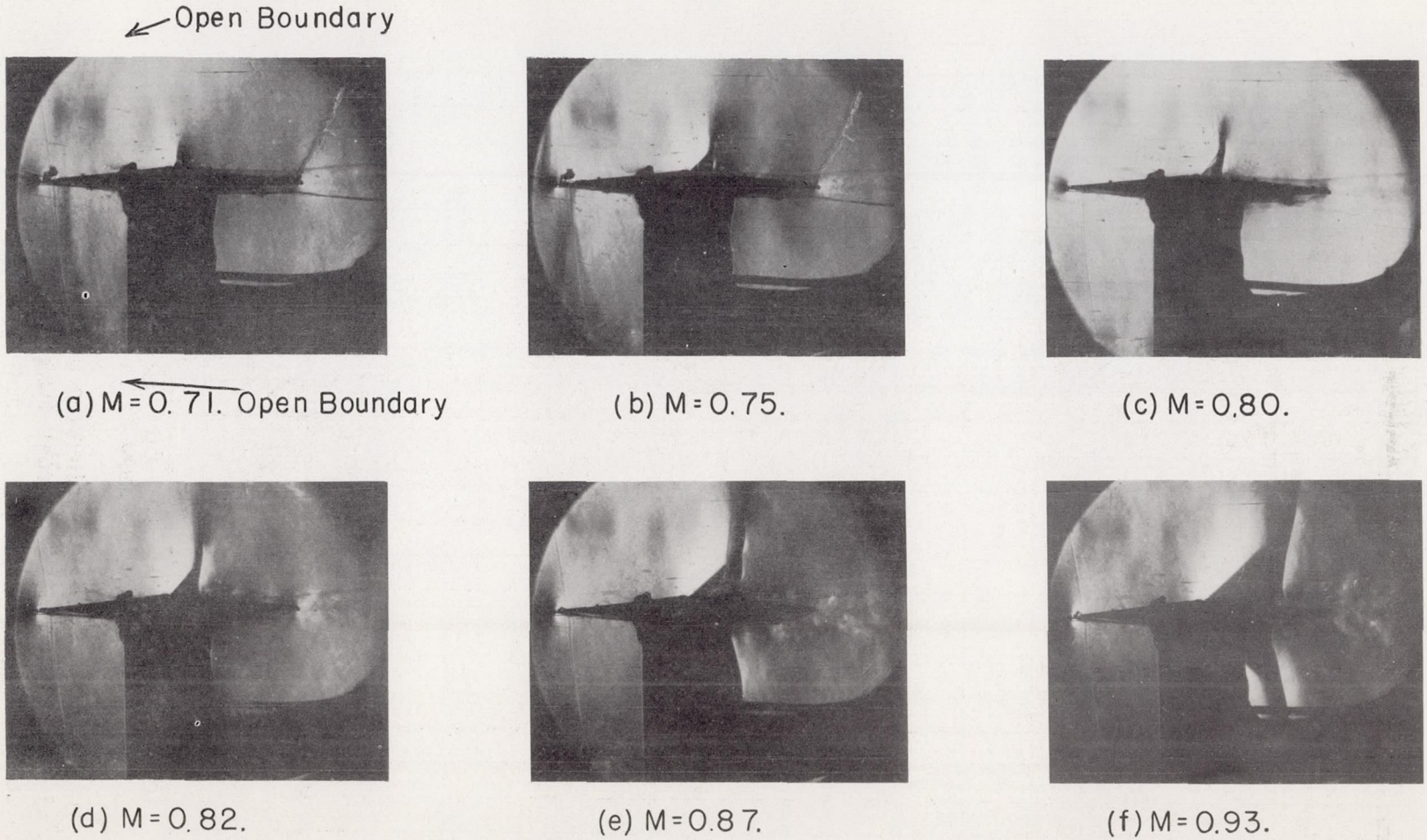

Figure 6.- Schlieren photographs of flow over a 10-percent-thick diamond airfoil in the open-throat tunnel.

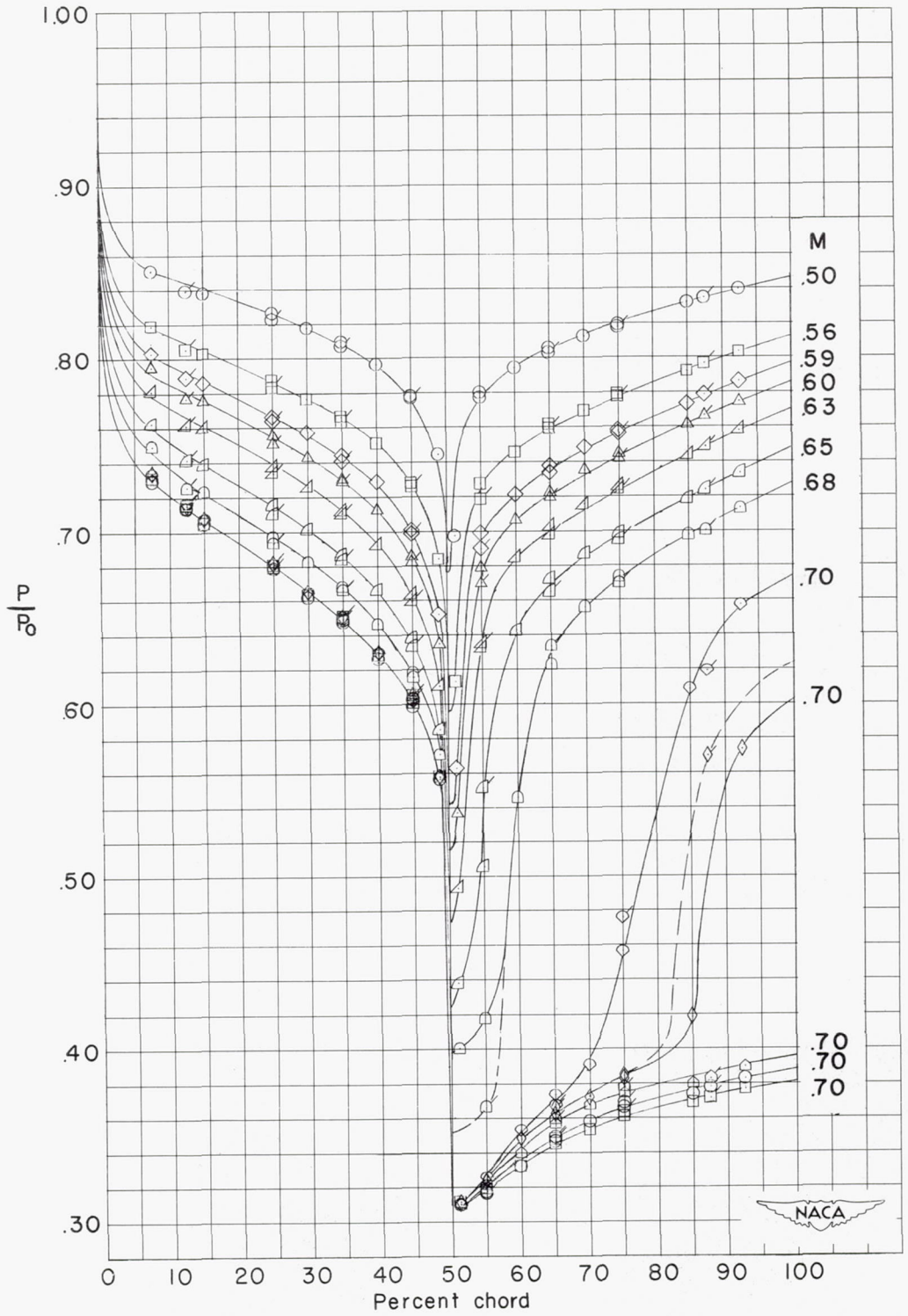

Figure 7.- Chordwise pressure distribution over a 10-percent-thick diamond airfoil in the closed throat tunnel. (Flagged symbols refer to lower surface.)

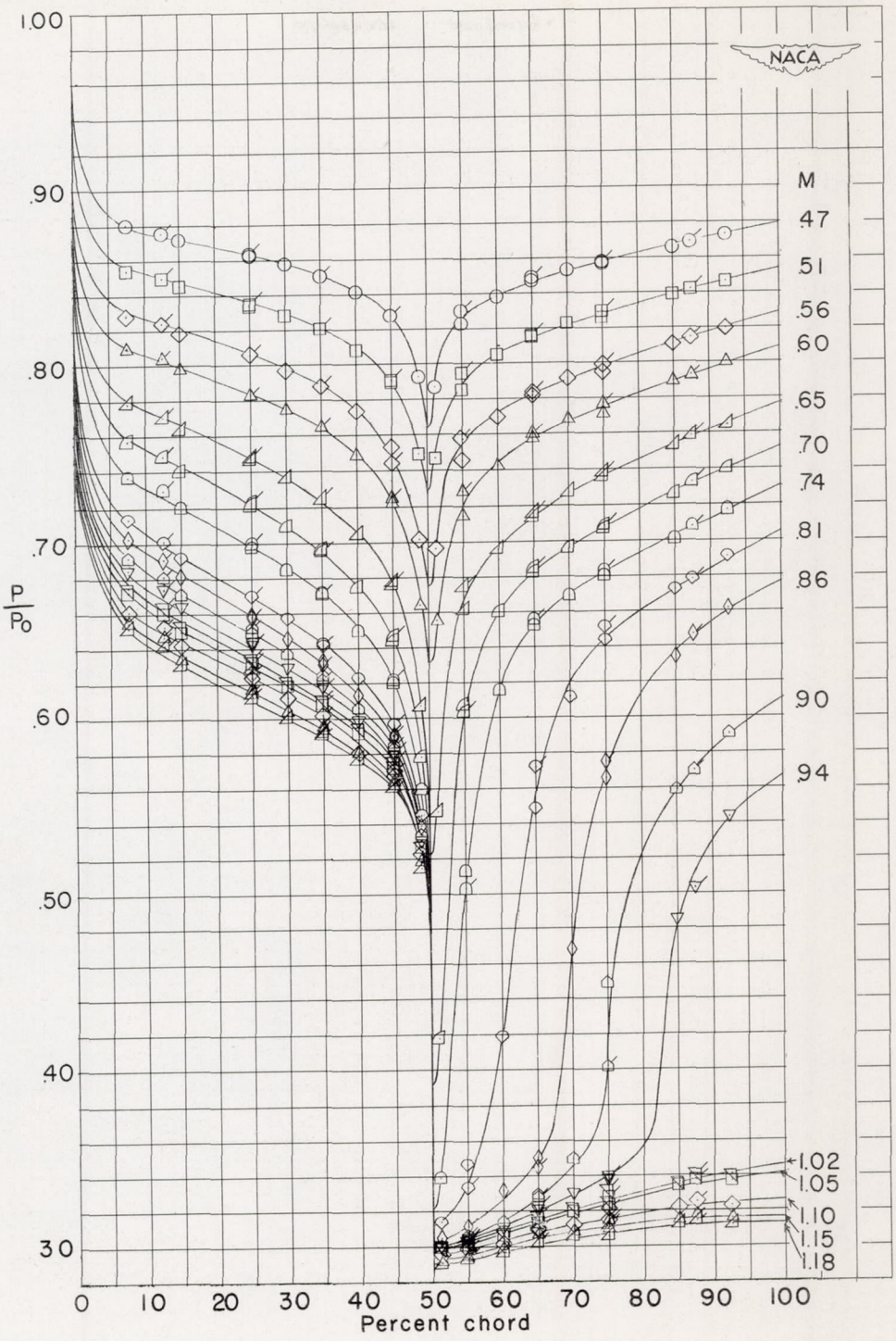

Figure 8.- Chordwise pressure distribution over a 10-percent-thick diamond airfoil in the $\frac{1}{8}$-open multiple-slotted throat tunnel. (Flagged symbols refer to lower surface.)

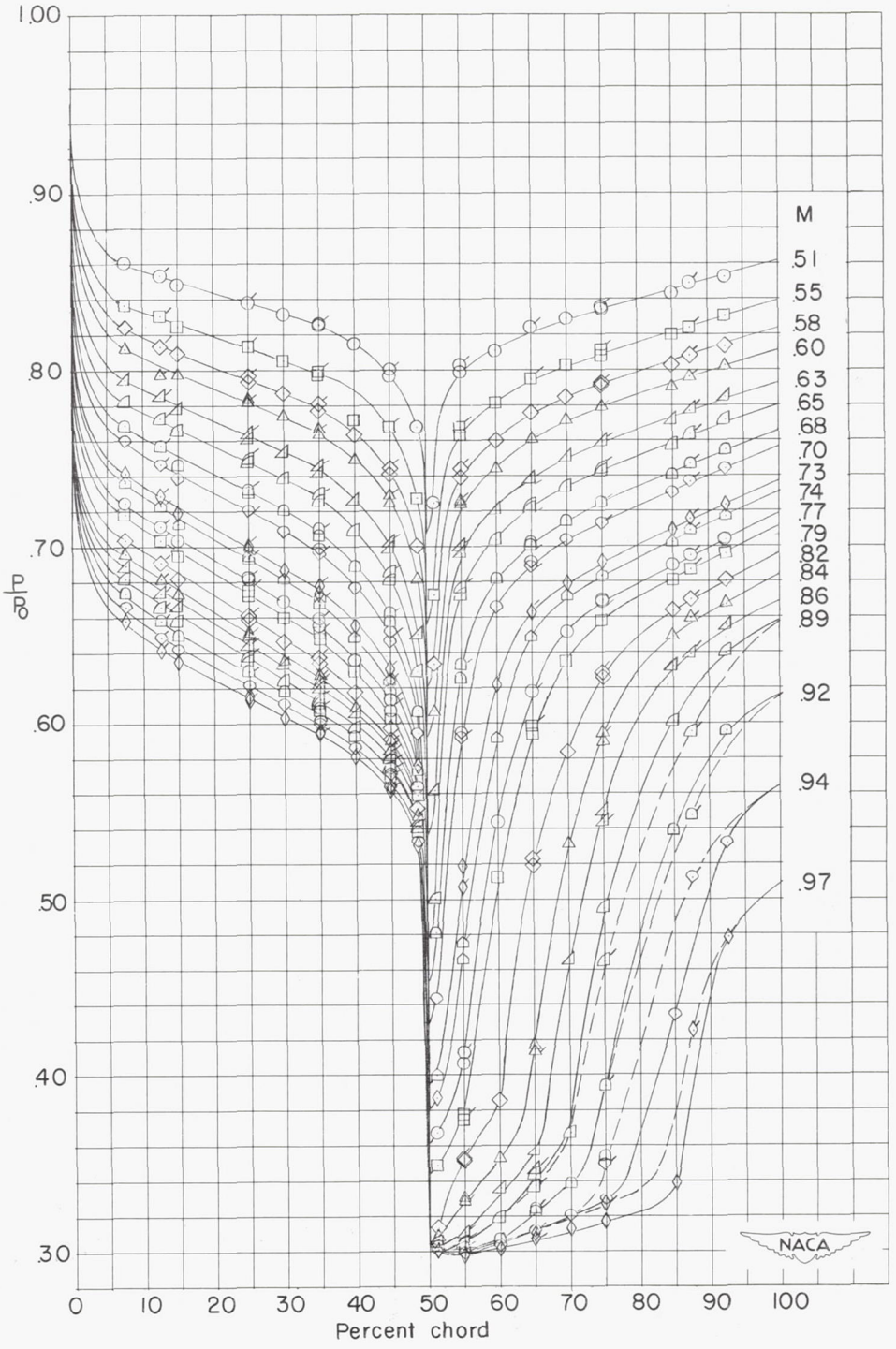

Figure 9.- Chordwise pressure distribution over a 10-percent-thick diamond airfoil in the $\frac{1}{5}$-open multiple-slotted throat tunnel. (Flagged symbols refer to lower surface.)

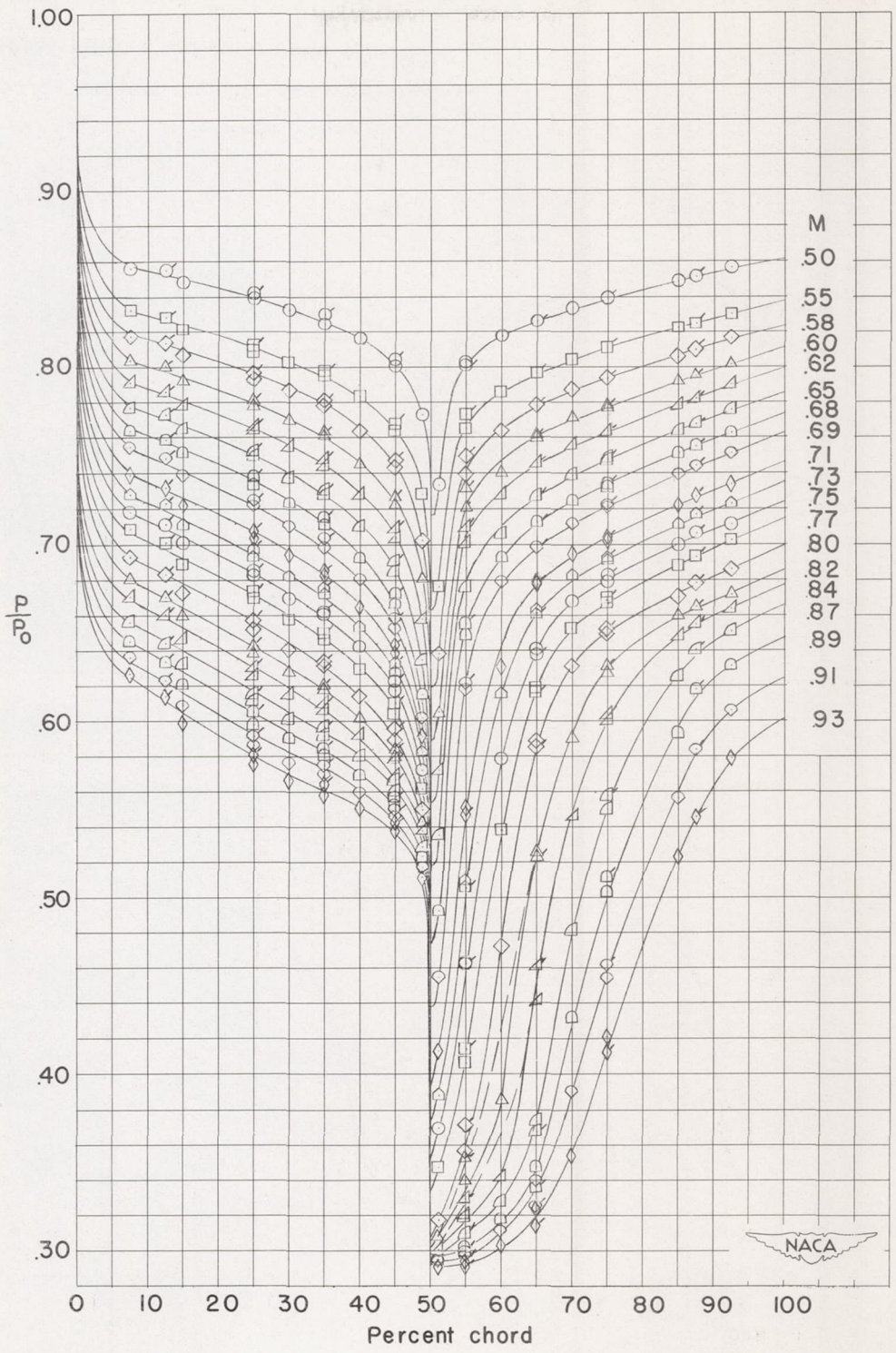

Figure 10.- Chordwise pressure distribution over a 10-percent-thick diamond airfoil in the open-throat tunnel. (Flagged symbols refer to lower surface.)

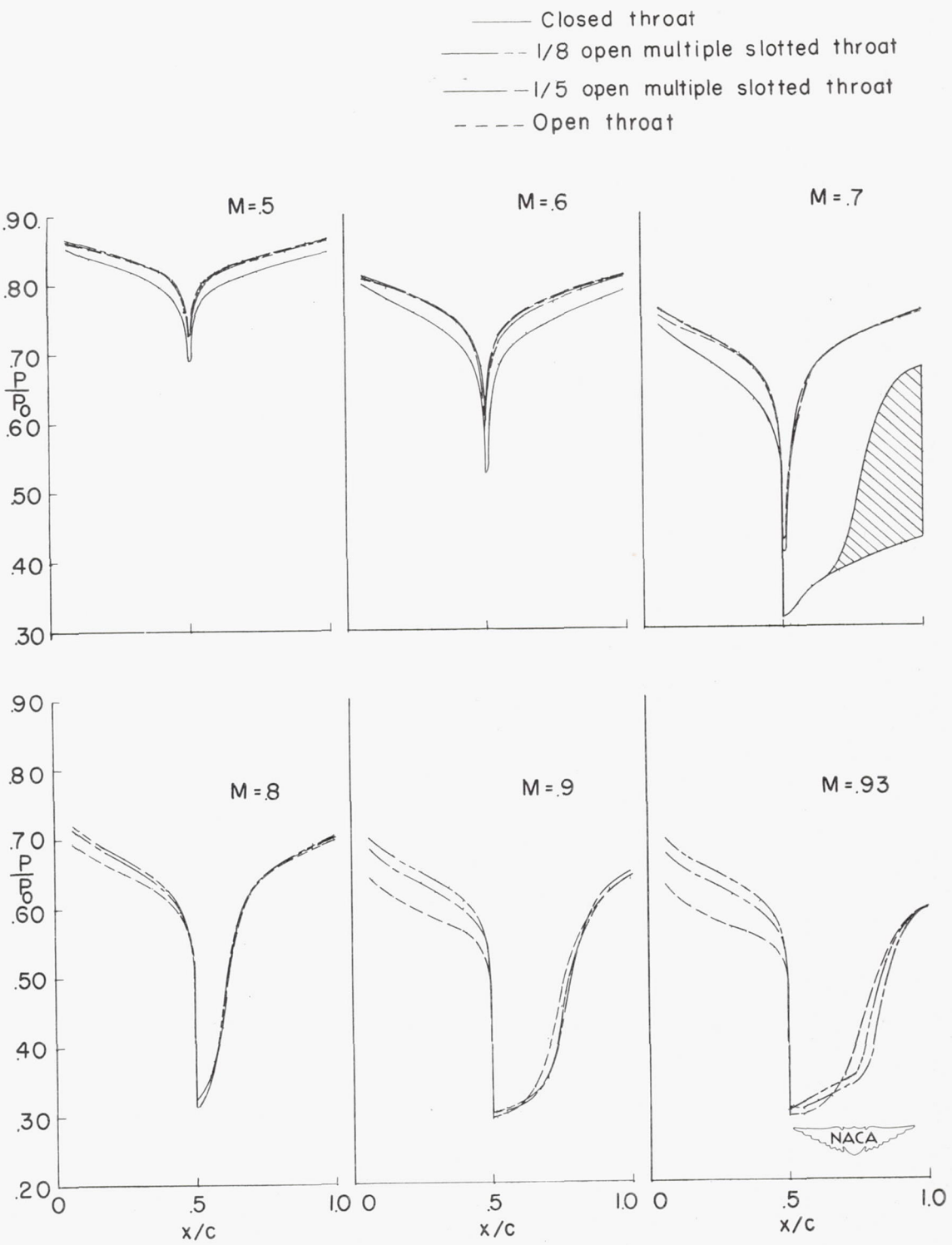

Figure 11.- Interpolated chordwise pressure distributions over a 10-percent-thick diamond airfoil in throats which have different boundaries at constant Mach numbers.

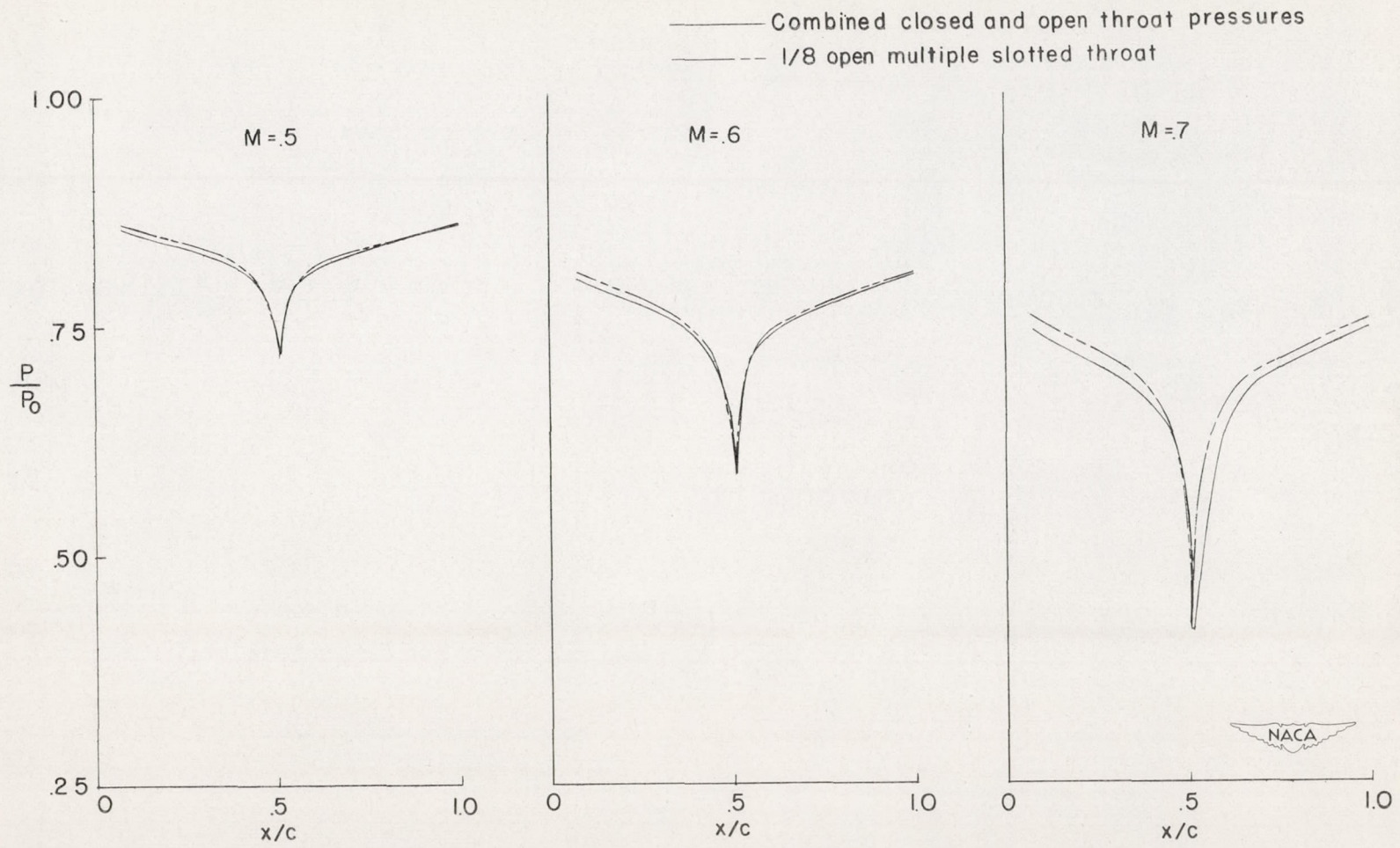

Figure 12.- Combined pressures over a 10-percent-thick diamond airfoil obtained in closed and open-throat tests as compared with uncorrected pressures obtained in $\frac{1}{8}$-open multiple-slotted throat tests at constant Mach numbers.

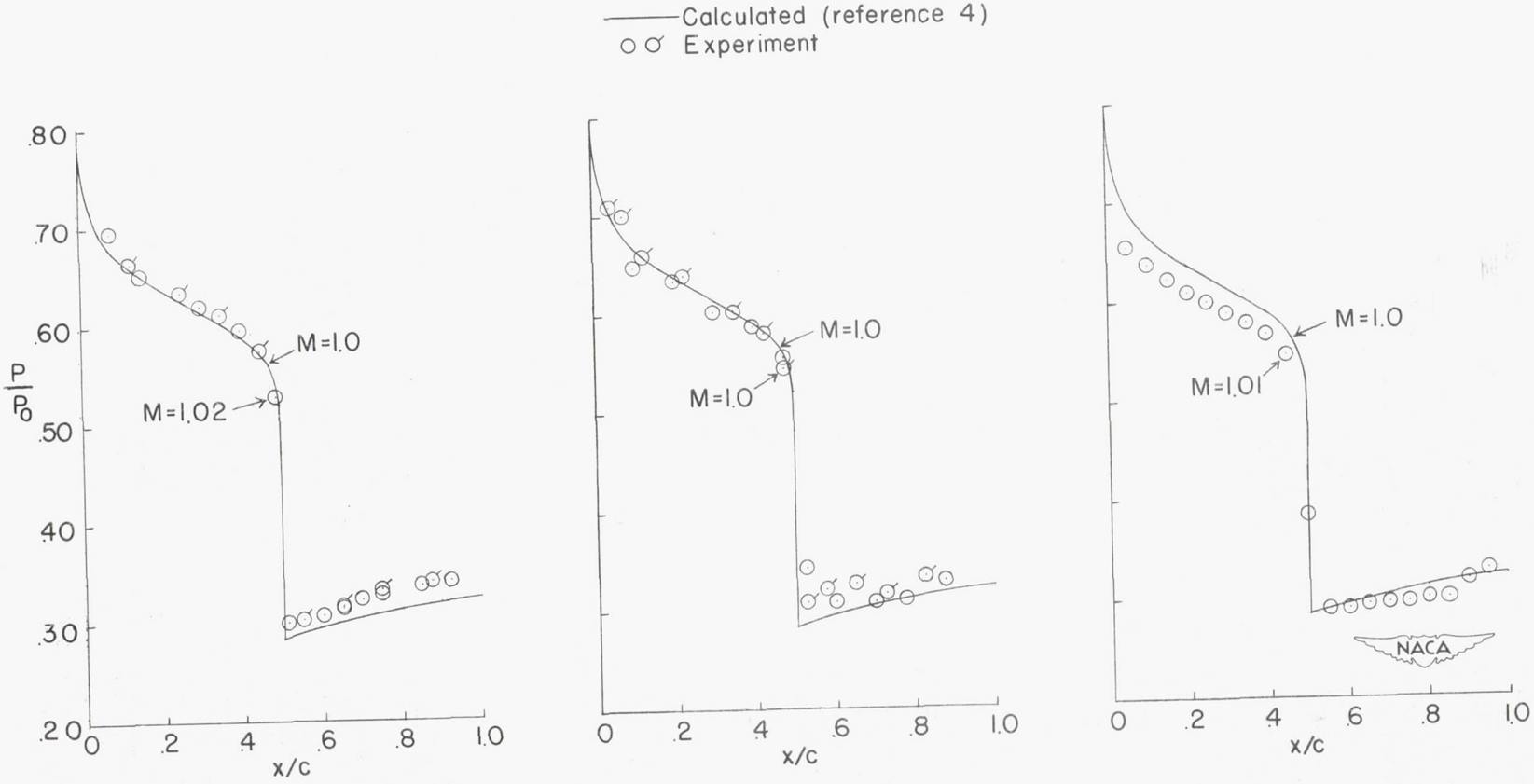

(a) $\frac{1}{8}$-open slotted throat tests.

(b) Langley annular transonic tunnel tests.

(c) Langley 4- by 19-inch tunnel tests.

Figure 13.- Comparison of calculated and experimental pressure distributions at $M \approx 1.0$.

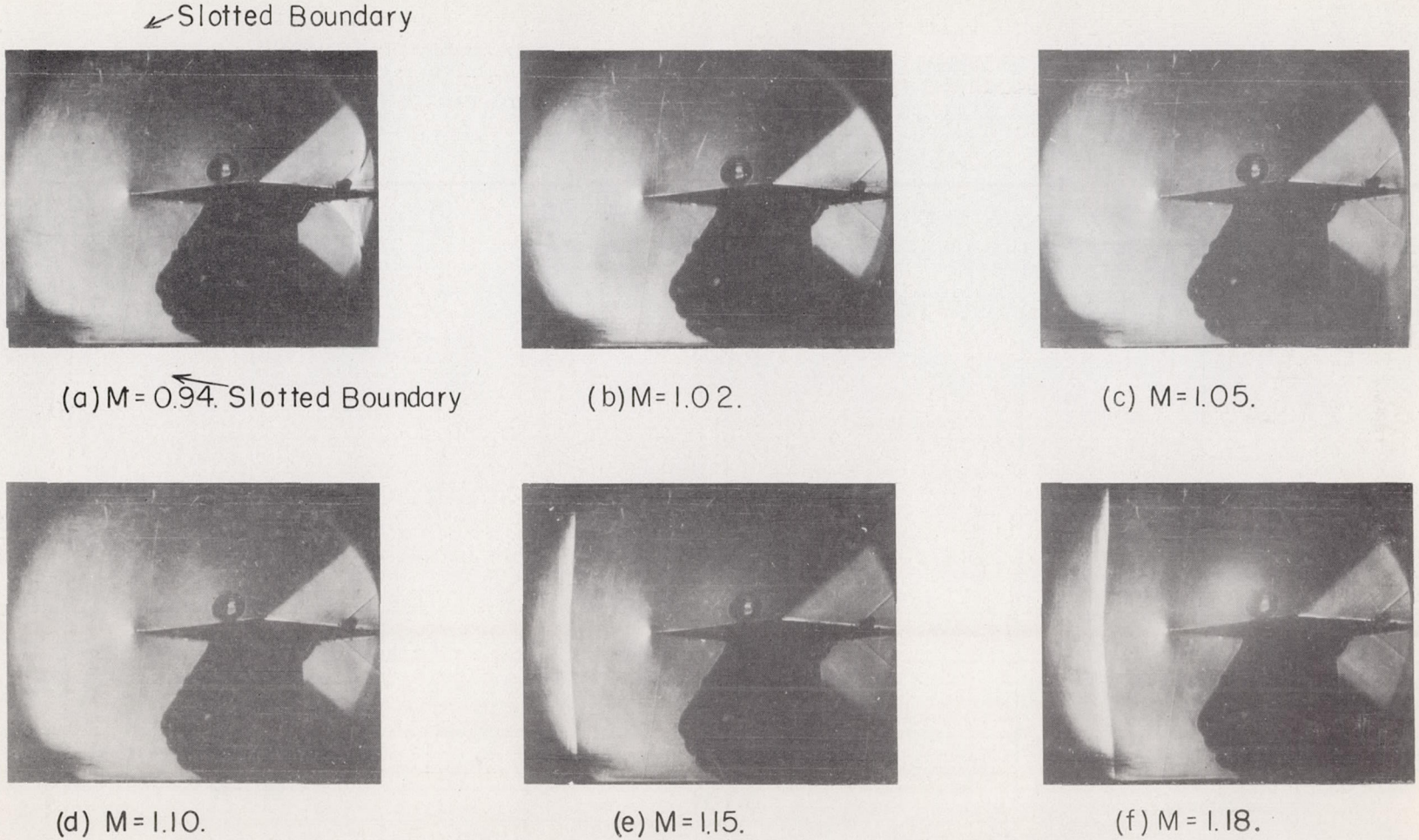

Figure 14.- Schlieren photographs of the flow over a 10-percent-thick diamond airfoil in the $\frac{1}{8}$-open multiple-slotted throat tunnel.

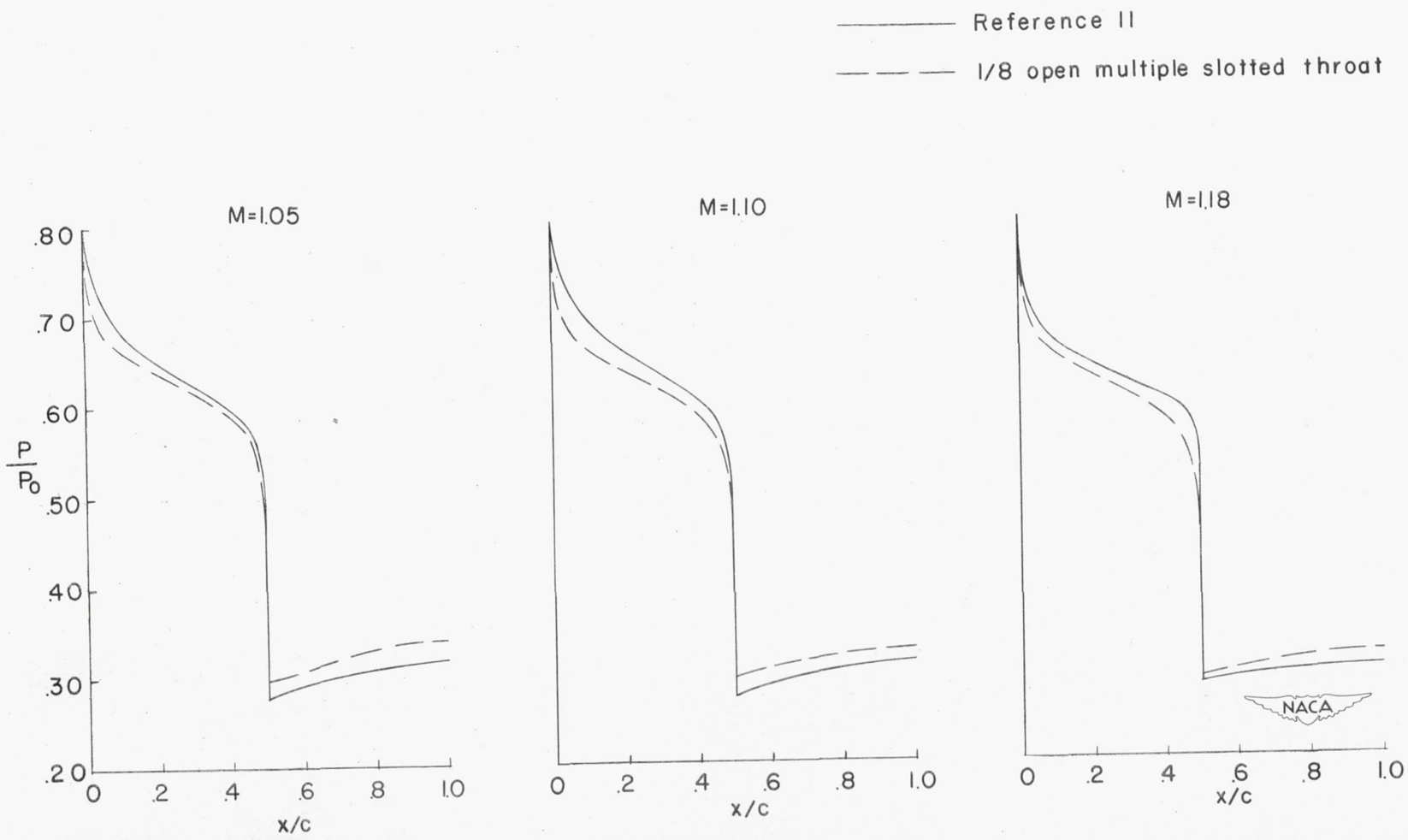

Figure 15.- Airfoil pressure distributions obtained in the $\frac{1}{8}$-open multiple-slotted throat as compared with the calculated pressure distributions.

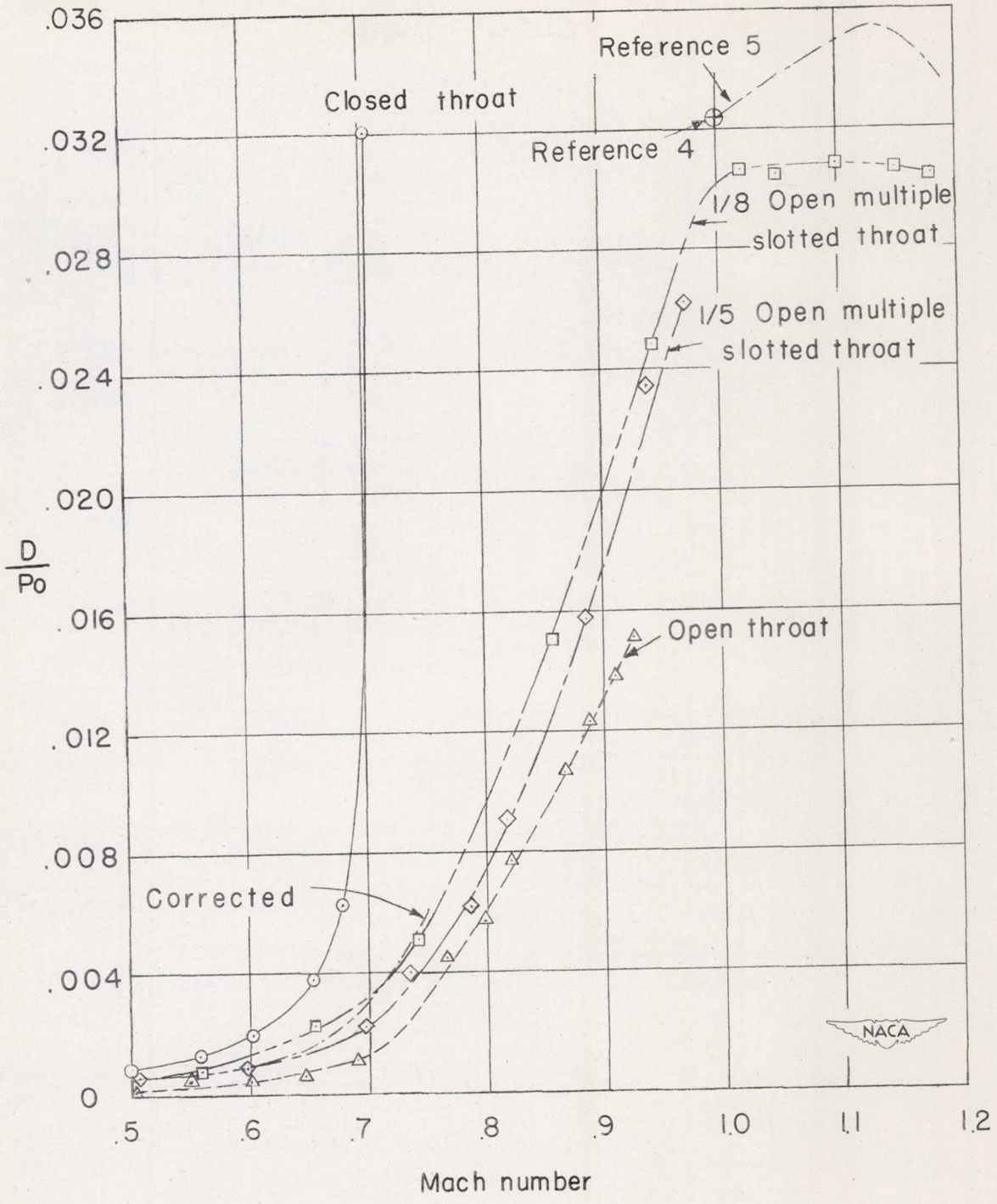

Figure 16.- Pressure drag curves of a 10-percent-thick diamond airfoil in throats which have different boundaries plotted against Mach number.

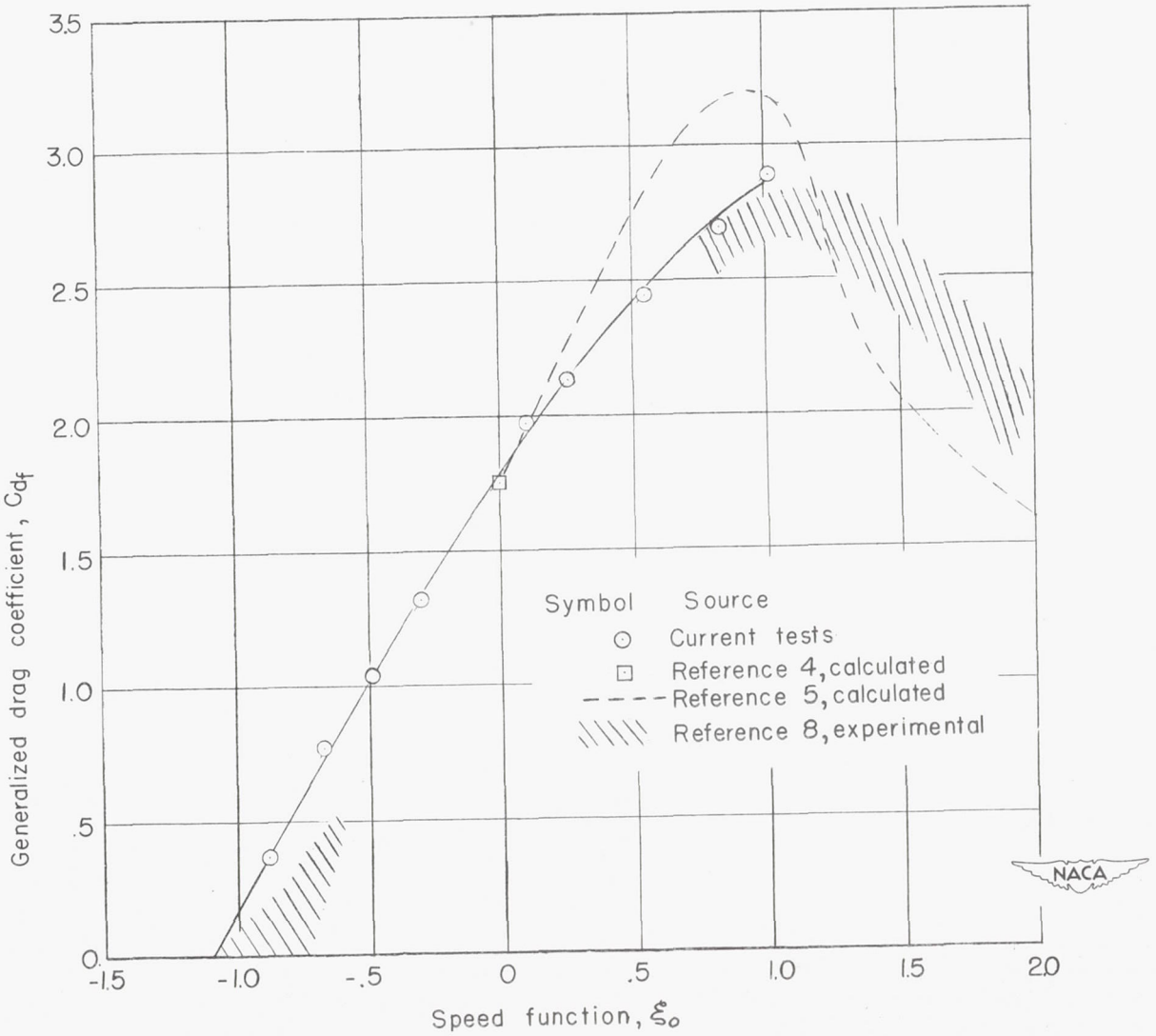

Figure 17.- Comparison of pressure drag of front half of profile obtained in $\frac{1}{8}$-open slotted-tunnel tests with theory and available experiment.

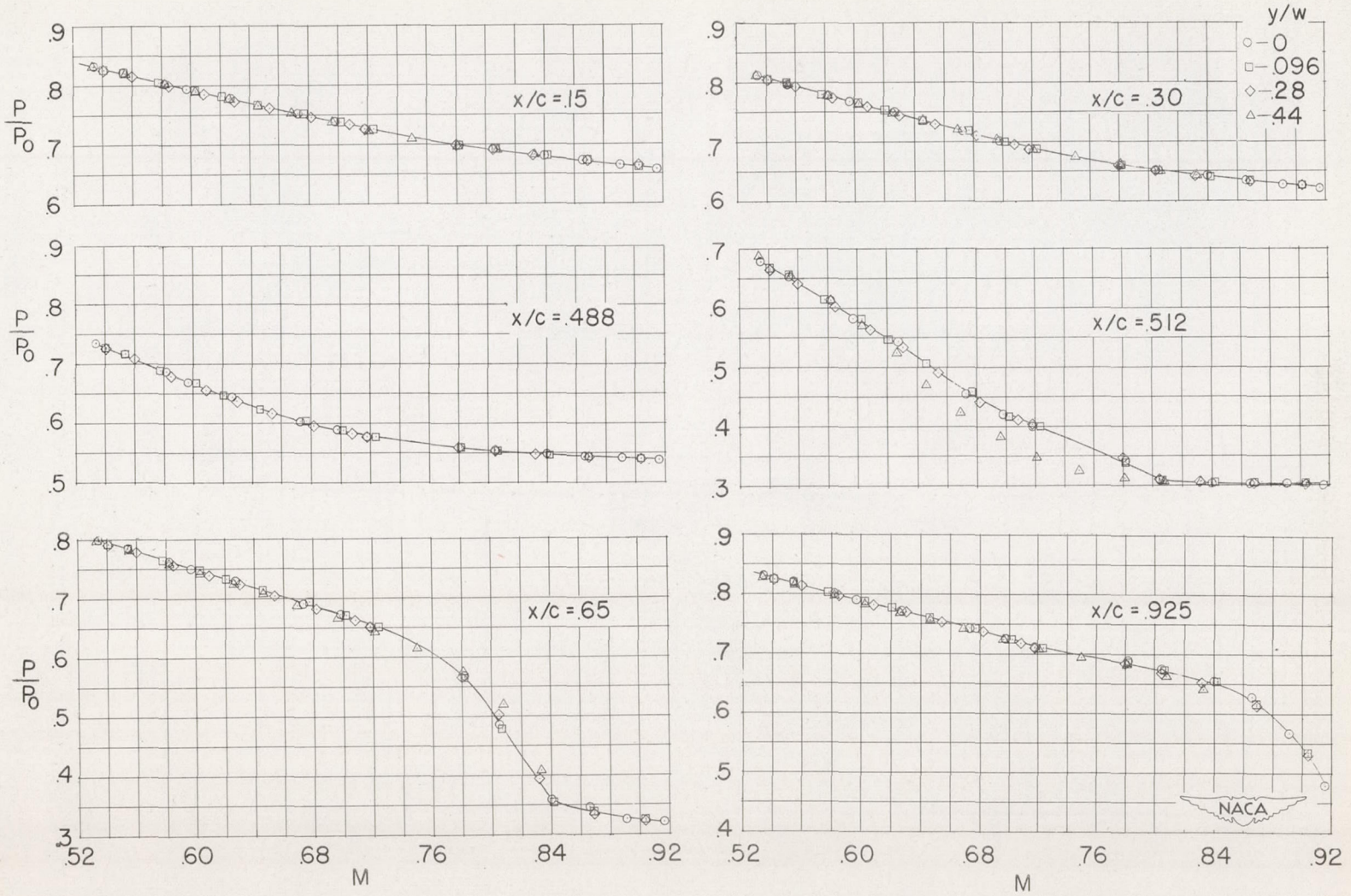

Figure 18.- Airfoil pressures for constant x/c at four spanwise positions against Mach number.

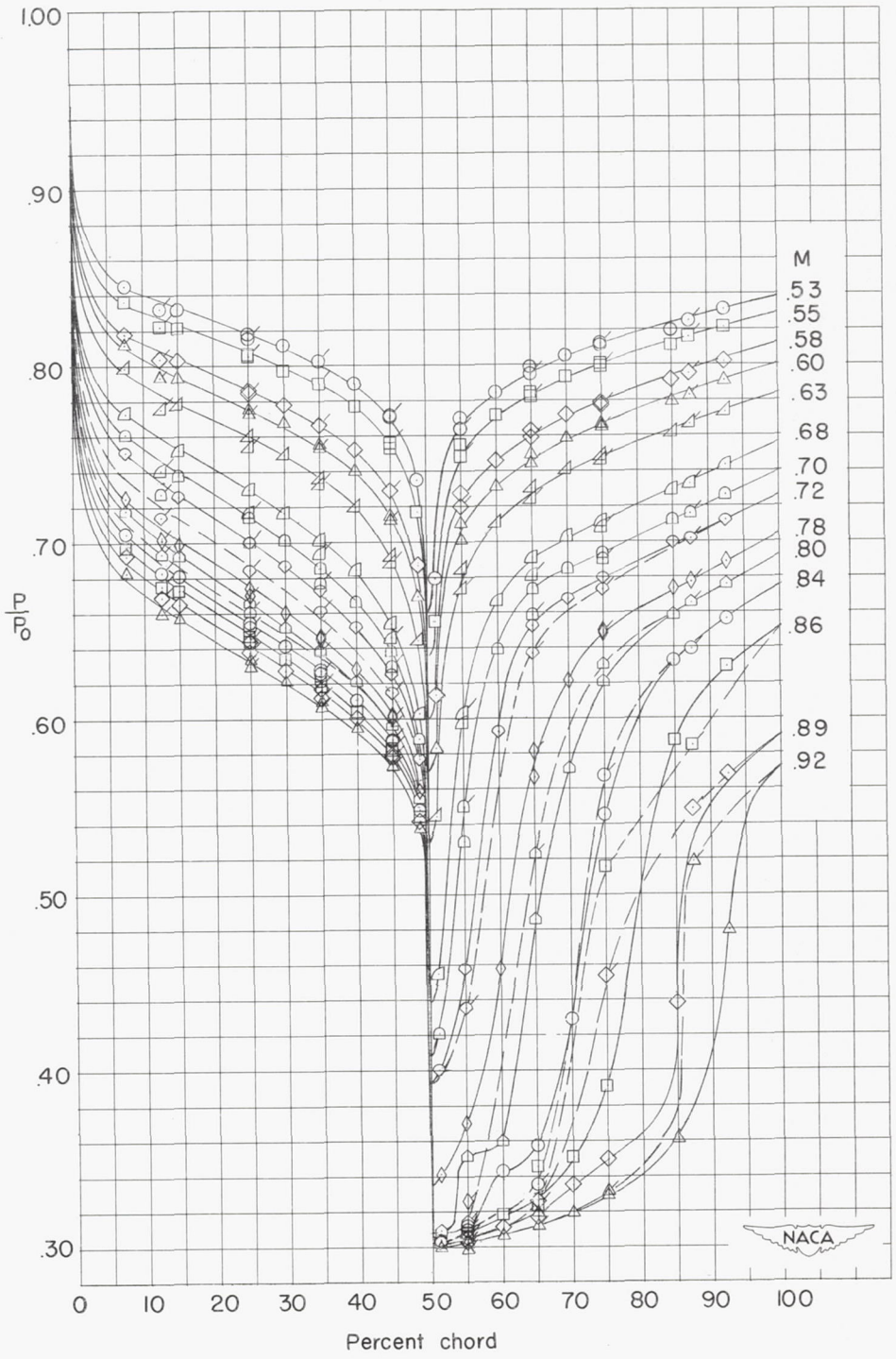

Figure 19.- Chordwise pressure distributions over a 10-percent-thick diamond airfoil in the $\frac{1}{5}$-open single-slotted throat tunnel. (Flagged symbols refer to lower surface.)

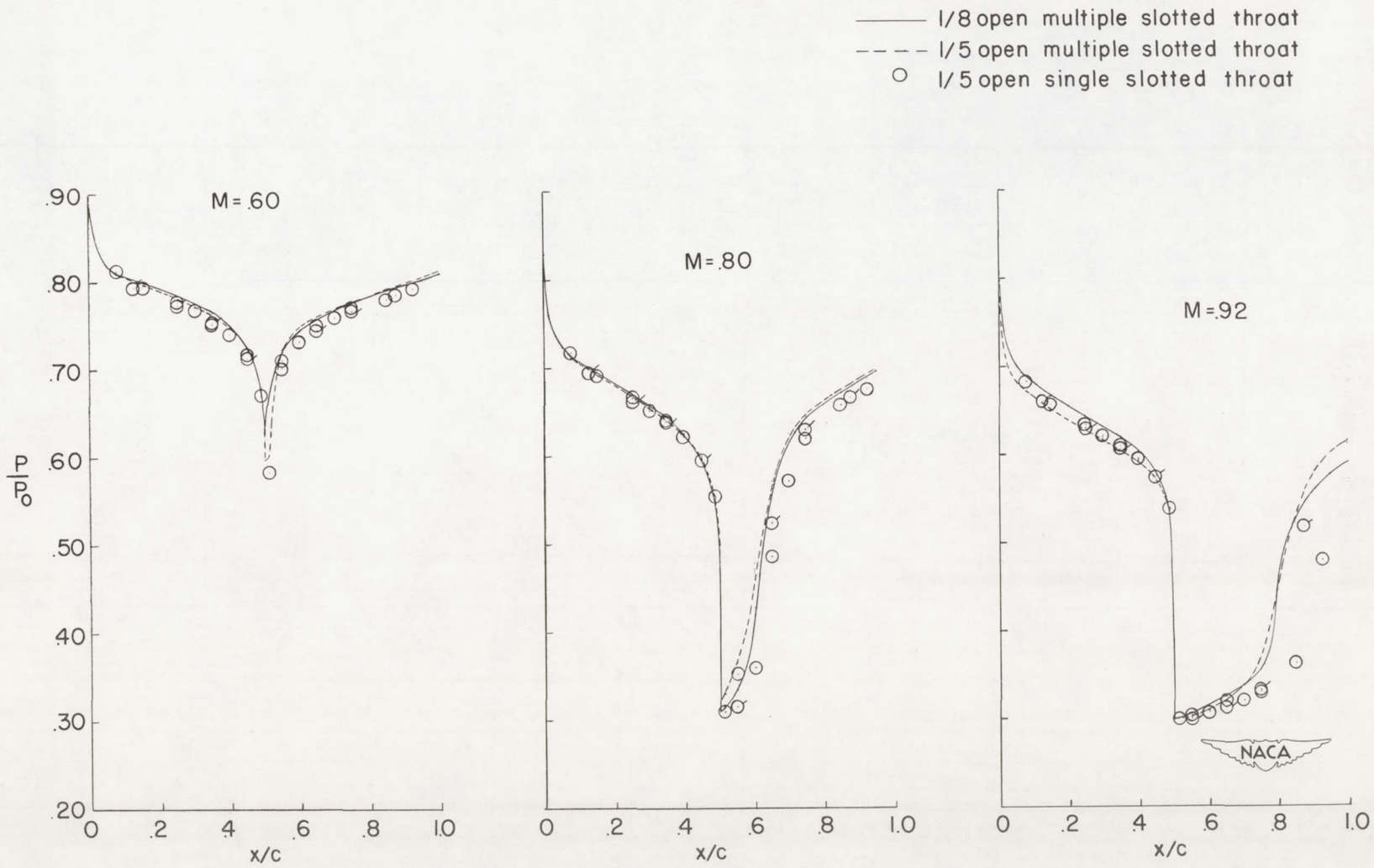

Figure 20.- Interpolated chordwise pressure distributions over a 10-percent-thick diamond airfoil in single- and multiple-slotted throats.

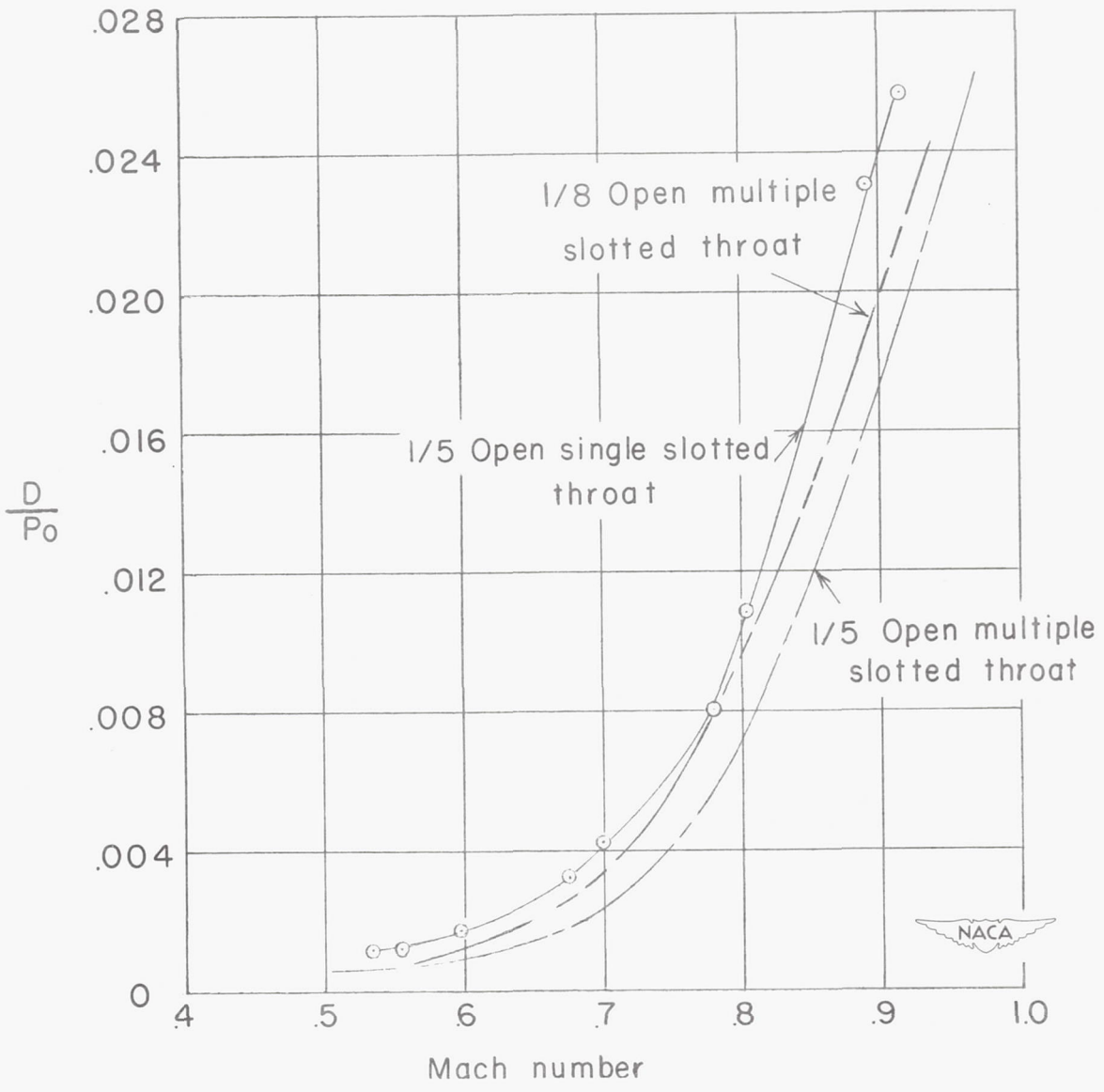

Figure 21.- Pressure drag curves of a 10-percent-thick diamond airfoil in single- and multiple-slotted throats with the same geometric open area.